Yep, J. Luminescence 3, 175 (1970).
[4]W. Schairer and T. O. Yep, Solid State Commun. 9, 421 (1971).
[5]For example, see P. J. Dean, Phys. Rev. 157, 655 (1967).
[6]D. Bimberg, thesis (Frankfurt, 1971) (unpublished).
[7]D. Bimberg (unpublished). The earlier gap assignment made by M. A. Gilleo, P. T. Bailey, and D. E. Hill, Phys. Rev. 174, 898 (1968), on the basis of luminescence experiments is incorrect; see M. A. Gilleo, P. T. Bailey, and D. E. Hill, Phys. Rev. B 3, 3581 (1971). But the new value of E_g differs only slightly from the earlier one.
[8]M. B. Panish and H. C. Casey, Jr., J. Appl. Phys. 40, 163 (1969).
[9]F. E. Williams and H. J. Eyring, J. Chem. Phys. 15, 289 (1947).

PHYSICAL REVIEW B VOLUME 4, NUMBER 10 15 NOVEMBER 1971

High-Frequency Damping in a Degenerate Electron Gas*

Arnold J. Glick
Center for Theoretical Physics and Department of Physics and Astronomy, University of Maryland, College Park, Maryland 20742

and

William F. Long
Indiana University, Bloomington, Indiana 47401

(Received 14 May 1971)

A closed form has been derived for the dissipative part of the complex frequency- and wave-number-dependent dielectric constant of a degenerate electron gas, $\epsilon(\vec{k}, \omega)$, valid in the limit $\omega \gg E_0$, $k < k_0$, where E_0 is the Fermi energy and k_0 the Fermi wave number. For $\omega > 2E_0$ this expression gives values of $\mathrm{Im}\epsilon(\vec{k}, \omega)$ which are in excellent agreement with the results of more detailed calculations in which the difficult integrals over phase space were performed by a Monte Carlo method. The formula also appears to give good numerical estimates of $\mathrm{Im}\epsilon(\vec{k}, \omega)$ for smaller values of ω (but $\omega > kk_0/m$), though its accuracy is not assured in that region. For example, in aluminum at the plasmon frequency, the asymptotic form agrees with the calculations of DuBois and Kivelson. The high-frequency formula derived may, therefore, be used to circumvent difficult numerical work in estimating the importance of electron correlation effects at high frequencies.

I. INTRODUCTION

If the random-phase approximation (RPA) is used to study the properties of a degenerate electron gas at zero temperature, [1] then one finds that the imaginary part of the frequency- and wave-number-dependent dielectric constant vanishes for frequencies above a certain cutoff:

$$\epsilon_2^{\mathrm{RPA}}(\vec{k}, \omega) = 0 \quad \text{for } \omega \geq kv_0(1 + k/2k_0). \tag{1}$$

Here v_0 and k_0 are the Fermi velocity and wave number, respectively. The contributions to $\epsilon_2(\vec{k}, \omega)$ at higher frequencies come from multiple-particle excitations in which there are at least two particles simultaneously excited out of the Fermi sea and sharing energy $\hbar\omega$. Several investigations of such multiple-particle terms have been reported, [2-4] culminating in Ref. 4 (referred to henceforth as DK), in which DuBois and Kivelson include contributions from diagrams in which dissipation is due to the production of two particle-hole pairs. DK account for dynamic screening in the interaction between the electrons, and find that earlier calculations are incomplete in that they include dynamic screening, but overlook certain "triangle graphs" which enter to the same order. DK's results are summarized in Eq. (3.18) of Ref. 4 as a two-dimensional integral over a complicated integrand. The only numerical results that they report are for the damping at the plasmon frequency over a range of electron density.

In the present paper we have used a simpler model for the damping and have derived a closed form for the imaginary part of the dielectric constant valid for frequencies much greater than the Fermi energy E_0. By comparison with detailed Monte Carlo calculations it is found that the asymptotic expression gives excellent agreement for $\omega > 2E_0$ and provides an order-of-magnitude estimate for smaller values of ω even fairly close to the RPA cutoff, Eq. (1).

II. FORMALISM

The calculation of the dielectric constant is carried out using the notation and formalism of Ref. 5, which is briefly reviewed here for completeness.

The fundamental equation for calculation of the longitudinal dielectric constant $\epsilon(\vec{k}, \omega)$ is

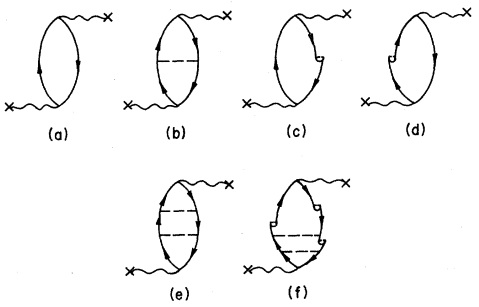

FIG. 1. Contributions to $\epsilon_2(\vec{k}, \omega)$ which vanish at high frequencies.

$$\mathrm{Im}\frac{1}{\epsilon(\vec{k}, \omega)} = -\frac{v(k)}{\Omega}\,\mathrm{Re}\int_0^\infty dt(e^{i\omega t} - e^{-i\omega t}) \times\langle\Psi_0 \mid \rho_{\vec{k}}^\dagger(t)\,\rho(0) \mid \Psi_0\rangle . \quad (2)$$

Here ω and $\vec{k}$ are the frequency and wave number, respectively, $v(\vec{k})$ is the Fourier transform of the interparticle potential, Ω is the quantization volume, $|\Psi_0\rangle$ is the many-particle ground state (in the Heisenberg representation), and $\rho_{\vec{k}}(t)$ is the Heisenberg fluctuation operator

$$\rho_{\vec{k}} = \int d\vec{r}\,\rho(\vec{r})\,e^{i\vec{k}\cdot\vec{r}} ,$$
$$\rho_k(t) = e^{iHt}\,\rho_{\vec{k}}\,e^{-iHt} ,$$

where $\rho(\vec{r})$ is the particle-density operator. The matrix element $\langle\Psi_0 \mid \rho_k^\dagger(t)\,\rho_k(0) \mid \Psi_0\rangle$ can be evaluated using many-body perturbation theory with terms represented by Feynman-type graphs. However, it is more convenient to first break the complex dielectric constant up into real and imaginary parts ϵ_1 and ϵ_2. Then

$$\epsilon_2(\vec{k}, \omega) = \frac{v(\vec{k})}{\Omega}\,\mathrm{Re}\int_0^\infty dt\,(e^{i\omega t} - e^{-i\omega t}) \times\langle\Psi_0 \mid \rho_k^\dagger(t)\,\rho_{\vec{k}}(0) \mid \Psi_0\rangle_B , \quad (3)$$

and the real part is related to the imaginary part by the Kramers-Kronig relation

$$\epsilon_1(\vec{k}, \omega) = 1 + \frac{2}{\pi}\,P\int_0^\infty \frac{\omega'\epsilon_2(\vec{k}, \omega')}{\omega'^2 - \omega^2}\,d\omega' . \quad (4)$$

In this paper interest will be focused one evaluation of Eq. (3), the imaginary component of the dielectric constant which may be directly related to energy dissipation.

The subscript B on the matrix element in (3) means that only "bubble" graphs are to be included. Bubble graphs are those which cannot be separated into two parts by severing one dotted line. Typical graphs which contribute to $\epsilon_2(\vec{k}, \omega)$ are shown in Figs. 1 and 2. These diagrams may be thought of as representing processes in which a density fluctuation causes the excitation of one or more particle-hole pairs which may interact via the Coulomb potential and finally deexcite into another density fluctuation.

III. HIGH-FREQUENCY CONTRIBUTIONS

The lowest-order graph, Fig. 1(a), reproduces the RPA to the dielectric constant, which was first found by Lindhard.[6] DuBois[2] studied the first-order terms shown in Figs. 1(b)–1(d). Glick[7] and Osaka[8] independently studied higher-order terms including those of the type shown in Figs. 1(e) and 1(f), but in all these cases the intermediate states (between the successive applications of the two-body force, denoted by dashed lines in the graphs) consist of exactly one particle and one hole. Consequently, phase-space limitations force $\epsilon_2(\vec{k}, \omega)$ to vanish for high frequencies as in Eq. (1).

Geldart and Vosko[9] showed that certain graphs with multiple-particle-hole excitations, analogous to Figs. 2(a) and 2(b), must be included to obtain consistent low-frequency results, and in particular to obtain a value for $\epsilon_1(\vec{k}, 0)$ which is consistent with the compressibility sum rule.[1] Here and in DK one is interested in high-frequency behavior, in which case it is necessary to include a whole class of multiple-particle-hole terms as shown in Fig. 2. These terms all contribute to the same order and are the lowest terms of perturbation theory which can give rise to damping in the high-frequency region.

DK use the full RPA dynamically screened interaction between electrons for their calculations. Since dynamic effects arise from the successive excitation and deexcitation of particle-hole pairs, consistency requires that they also include certain "triangle graphs" to account for the possibility that one of the particle-hole pairs in the intermediate state is associated with the dynamic interaction.

In the present paper we report calculations for

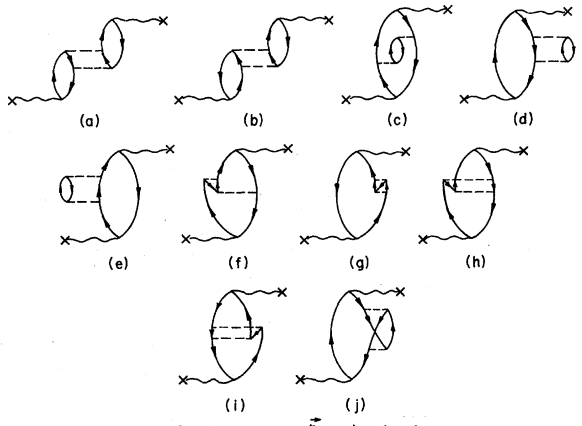

FIG. 2. Contributions to $\epsilon_2(\vec{k}, \omega)$ which give nonzero dissipation at high frequencies.

an electron gas interacting via a static screened Coulomb force. Consequently the triangle graphs are not included. They would consistently enter as a higher-order correction along with other terms.

Geldart and Vosko[9] in their calculation of $\epsilon(k, 0)$ have shown that using static forces for the intermediate interactions can give results which differ by as much as a factor of 2 from those obtained with dynamic forces. When applied to $\epsilon(\vec{k}, \omega)$ for large ω, one might expect that the intermediate interactions would also carry higher frequencies and hence the static and dynamic calculations could differ by an even greater amount. However, comparison of our numerical results with those of DK shows that at metallic densities and in the neighborhood of the plasma frequency the two calculations differ by no more than in the low-frequency case, while in the limit of very high frequencies screening becomes unimportant and the two calculations become equivalent.

We first study the high-frequency limit. Throughout this paper we consider k fixed and small compared to the Fermi wave number k_0. For very high frequencies the two particles in the intermediate state have energies approximately equal to $\frac{1}{2}\omega$, since the hole states are restricted to beneath the Fermi surface and hence have relatively little energy. In this case the intermediate interactions are of the form

$$\nu(\vec{q}, \tfrac{1}{2}\omega) = v(\vec{q})/\epsilon(\vec{q}, \tfrac{1}{2}\omega), \tag{5}$$

where q is the momentum transferred through the interaction. The dynamically screened interaction reduces to the unscreened case in the high-frequency limit because

$$\lim \epsilon(\vec{q}, \omega) = 1 \quad \text{as } \omega \to \infty. \tag{6}$$

The statically screened interaction that we use has the form

$$\nu(\vec{q}) = 4\pi e^2/(q^2 + \alpha), \tag{7}$$

where α is the screening constant given by

$$\alpha = 4k_0/\pi a_0 . \tag{8}$$

Conservation of energy and momentum relate $\vec{q}$ to ω, and in the limit one finds that $\pm\vec{q}$ are the approximate momenta of the particles and $q \sim (m\omega)^{1/2}$. Thus this interaction also reduces to the unscreened form in the high-frequency limit.

As we go to lower frequencies the screening becomes important. In the static treatment one omits the possibility of a coherent plasmon excitation in the intermediate state. As DK have pointed out, for frequencies up to the plasmon frequency ω_p there is insufficient energy to create intermediate plasmons. For very large ω there also are no intermediate plasmons because q is above the cutoff wave number. However, there is a frequency range from ω_p up to six or seven times the Fermi energy, where intermediate plasmons could augment the damping. Nevertheless, their contribution is not expected to be large. In any case the static calculation provides a lower limit to the damping.

The graphs considered are shown in Fig. 2. Graphs 2(f)–2(j) can be obtained from 2(a)–2(e) by the exchange of two particles entering one of the interactions. By an astute labeling of graphs one can combine these terms into the form[10]

$$\epsilon_2(\vec{k}, \omega) = \frac{32\pi^3 m\, v(\vec{k})}{\Omega^3} \sum_{\vec{k}_1, \vec{k}_2, \vec{k}_3} \eta_{\vec{k}_1 - \vec{k}_2 <}\, \eta_{\vec{k}_3 - \vec{k} <}\, \eta_{\vec{k}_1 >}\, \eta_{\vec{k}_3 - \vec{k}_2 >}\, \delta(m\omega - \vec{k}_{13}\cdot\vec{k}_2 - \vec{k}_3\cdot\vec{k} + \tfrac{1}{2}\vec{k}^2)$$
$$\times \sigma_1(\vec{k}_1, \vec{k}_2, \vec{k}_3, \vec{k}, \omega)\, \sigma_3(\vec{k}_1, \vec{k}_2, \vec{k}_3, \vec{k}, \omega), \tag{9}$$

where

$$\sigma_1(\vec{k}_1, \vec{k}_2, \vec{k}_3, \vec{k}, \omega) = \frac{m}{4\pi} \left(\frac{(\vec{k}_2\cdot\vec{k})\, \nu(\vec{k}_2)}{(\vec{k}_{13}\cdot\vec{k}_2)(\vec{k}_{13}\cdot\vec{k}_2 + \vec{k}_2\cdot\vec{k})} - \frac{(\vec{k}_2\cdot\vec{k} - \vec{k}^2)\, \nu(\vec{k}_2 - \vec{k})}{(\vec{k}_{13}\cdot\vec{k}_2 - \vec{k}_{13}\cdot\vec{k})(\vec{k}_{13}\cdot\vec{k}_2 - \vec{k}_{13}\cdot\vec{k} + \vec{k}_2\cdot\vec{k} - \vec{k}^2)} \right). \tag{10}$$

Note that $\vec{k}_1$ and $\vec{k}_3$ always enter the factor $\sigma_1(\vec{k}_1, \vec{k}_2, \vec{k}_3, \vec{k}, \omega)$ in the combination $\vec{k}_{13} \equiv \vec{k}_1 - \vec{k}_3$. The other factor $\sigma_3(\vec{k}_1, \vec{k}_2, \vec{k}_3, \vec{k}, \omega)$ accounts for both direct and exchange graphs. It can be obtained from $\sigma_1(\vec{k}_1, \vec{k}_2, \vec{k}_3, \vec{k}, \omega)$ by writing

$$\sigma_2(\vec{k}_1, \vec{k}_2, \vec{k}_3, \vec{k}, \omega) \equiv \sigma_1(\vec{k}_2 \longrightarrow -\vec{k}_{13}), \tag{11}$$

i.e., σ_1 with the vectors $\vec{k}_2$ and $-\vec{k}_{13}$ interchanged. Then

$$\sigma_3(\vec{k}_1, \vec{k}_2, \vec{k}_3, \omega) \equiv \sigma_1(\vec{k}_1, \vec{k}_2, \vec{k}_3, \vec{k}, \omega)$$
$$- \tfrac{1}{2}\, \sigma_2(\vec{k}_1, \vec{k}_2, \vec{k}_3, \vec{k}, \omega). \tag{12}$$

Now we describe how Eq. (9) was explicitly evaluated.

IV. NUMERICAL EVALUATION

The sums over $\vec{k}_1$, $\vec{k}_2$, and $\vec{k}_3$ in Eq. (9) can be converted to integrals in the usual manner. However, only the first few of the nine dimensions of the integral can be carried out simply using analytic means. This difficulty was overcome by num-

erically evaluating the integral using a Monte Carlo technique. The theorem applied was[11]

$$\epsilon_2(\vec{k},\omega)=\frac{4v(k)}{(2\pi)^6}\ \tau(\vec{k},\omega)\ \Sigma(\vec{k},\omega)\ , \tag{13}$$

where

$$\tau(\vec{k},\omega)\equiv m\int\int\int d\vec{k}_1\, d\vec{k}_2\, d\vec{k}_3 \times\delta(m\omega-\vec{k}_{13}\cdot\vec{k}_2-\vec{k}_3\cdot\vec{k}+\tfrac{1}{2}k^2) \times\eta_{\vec{k}_3-\vec{k}_2>}\ \eta_{\vec{k}_3-\vec{k}<}\ \eta_{\vec{k}_1>}\ \eta_{\vec{k}_1-\vec{k}_2<}\ , \tag{14}$$

which may be recognized as the phase-space integral for a system of two particles and two holes, and

$$\Sigma(\vec{k},\omega)\equiv\langle\langle\sigma_1(\vec{k}_1,\vec{k}_2,\vec{k}_3,\vec{k},\omega)\ \sigma_3(\vec{k}_1,\vec{k}_2,\vec{k}_3,\vec{k},\omega)\rangle\rangle_{\vec{k},\omega}, \tag{15}$$

where $\langle\langle\cdots\rangle\rangle_{\vec{k},\omega}$ denotes an average over the phase space of a system of two particles and two holes of total wave number $\vec{k}$ and frequency ω. To evaluate $\Sigma(\vec{k},\omega)$ a computer program was written which would generate random events in the appropriate phase space. Errors in the average $\Sigma(\vec{k},\omega)$ as measured by the standard deviation were generally held to less than 10%, but as $\omega\to kk_0/m$, the magnitude of the function in the double brackets varied too much over phase space to permit meaningful calculations. The phase-space integral $\tau(\vec{k},\omega)$ is itself difficult to evaluate and numerical procedures must be employed. The method chosen was a Monte Carlo algorithm which was a variant on that developed by Cerulus and Hagedorn.[12] The advantages of evaluating by a Monte Carlo method rather than making approximations which permit analytic evaluation of the quadratures are twofold: The exact form of $\sigma_1(\vec{k}_1,\vec{k}_2,\vec{k}_3,\vec{k},\omega)$ as given in Eq. (10) may be retained, thus eliminating the necessity for expansions in powers of k, and errors in the calculation may be accurately estimated by means of the Central Limit Theorem.

Typical results are shown by the dotted lines in Fig. 3, where they are compared with the asymptotic formulas derived in the next section.

V. ASYMPTOTIC FORMULAS

The geometrical constraints in Eq. (9) are those of two particle-hole pairs. One can exhibit this explicitly by introducing the variables

$$\vec{q}_1=\vec{k}_1-\vec{k}_2,\quad \vec{q}_2=\vec{k}_3-\vec{k},$$
$$\vec{q}_3=\vec{k}_1,\qquad \vec{q}_4=\vec{k}_3-\vec{k}_2,$$

using these variables and converting Eq. (9) to an integral,

$$\epsilon_2(\vec{k},\omega)=\frac{4mv(\vec{k})}{(2\pi)^6}\iiint d\vec{q}_1\, d\vec{q}_2\, d\vec{q}_3\, d\vec{q}_4\,\eta_{\vec{q}_1<}\,\eta_{\vec{q}_2<}\,\eta_{\vec{q}_3>}\,\eta_{\vec{q}_4>}\,\delta(m\omega+\tfrac{1}{2}\vec{q}_1{}^2+\tfrac{1}{2}\vec{q}_2{}^2-\tfrac{1}{2}\vec{q}_3{}^2-\tfrac{1}{2}\vec{q}_4{}^2) \times\delta^3(\vec{q}_1+\vec{q}_2-\vec{q}_3-\vec{q}_4+\vec{k})\ \sigma_1'(\vec{q}_1,\vec{q}_2,\vec{q}_3,\vec{q}_4,\vec{k},\omega)\ \sigma_3'(\vec{q}_1,\vec{q}_2,\vec{q}_3,\vec{q}_4,\vec{k},\omega)\ , \tag{16}$$

where σ_1' and σ_3' are the functions σ_1 and σ_3 expressed in terms of the new variables. In the high-frequency limit $\omega\gg E_0$ the magnitudes of the integration variables satisfy $q_3, q_4\gg k_0> q_1,\ q_2,\ k$, and also $q_3\simeq q_4\simeq(m\omega)^{1/2}$. In this limit

$$\sigma_1'(\vec{q}_1,\vec{q}_2,\vec{q}_3,\vec{q}_4,\vec{k},\omega)\simeq\frac{k^2}{a_0(m\omega+\alpha)(m\omega)^2} \times\left[1-2\mu^2\left(1+\frac{m\omega}{m\omega+\alpha}\right)\right], \tag{17}$$

where

$$\mu\equiv(\vec{q}_3\cdot\vec{k})/(|\vec{q}_3||\vec{k}|).$$

Substituting into Eq. (9) gives

$$\epsilon_2(\vec{k},\omega)\simeq\frac{k^2}{8\pi^5a_0^3(m\omega)^4(m\omega+\alpha)^2}\int_0^{k_0}d\vec{q}_1\int_0^{k_0}d\vec{q}_2 \times\int_0^{\infty}d\vec{q}_3\int_0^{\infty}d\vec{q}_4\ \delta(m\omega-\tfrac{1}{2}\vec{q}_3{}^2-\tfrac{1}{2}\vec{q}_4{}^2) \times\delta^3(\vec{k}-\vec{q}_3-\vec{q}_4)\left[1-2\mu^2\left(1+\frac{m\omega}{m\omega+\alpha}\right)^2\right]^2. \tag{18}$$

The integrations are now easy and yield the result

$$\epsilon_2(\vec{k},\omega)=\frac{4}{9}\ \frac{k_0^6}{\pi^2a_0^3}\ \frac{k^2}{(m\omega)^{7/2}(m\omega+\alpha)^2} \times\left[\frac{7}{15}+\frac{4}{15}\ \frac{m\omega}{m\omega+\alpha}+\frac{4}{5}\left(\frac{m\omega}{m\omega+\alpha}\right)^2\right] \tag{19}$$

or, without screening,

$$\epsilon_2(\vec{k},\omega)=\frac{92}{135}\ \frac{k_0^6}{\pi^2a_0^3}\ \frac{k^2}{(m\omega)^{11/2}}\ . \tag{20}$$

VI. CONCLUSION

The results of the calculations are summarized by Figs. 3 and 4. Figure 3 shows $\epsilon_2(\vec{k},\omega)$ plotted as a function of frequency for a value of the Fermi wave number appropriate to aluminum. Consider the value of ϵ_2 at the plasma frequency. The results of DK were

$$\epsilon_2(\vec{k},\omega_p)=(3.4\times10^{-2})(k/k_0)^2 \text{ with dynamic screening}$$
$$=(5.6\times10^{-1})(k/k_0)^2 \text{ without screening.}$$

Our results using (9) and the Monte Carlo method

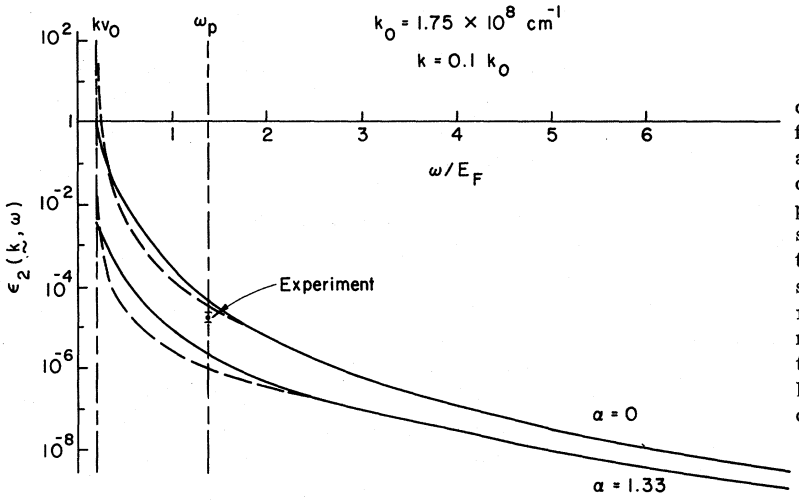

FIG. 3. Imaginary part of the dielectric constant is plotted as a function of ω/E_F for $k_0 = 1.75\times10^8$ cm^{-1} (appropriate to aluminum) and $k = 0.1k_0$. The dielectric constant is in units of $2k_0/a_0k^2$. The upper pair of curves are the results without screening ($\alpha = 0$) and the lower pair are the results including Thomas-Fermi screening (in units of k_F^2). Dashed lines represent the results of evaluating (9) by means of a Monte Carlo technique, while the solid lines are the asymptotic formulas (19) and (20) (the experimental point comes from Ref. 3).

are

$$\epsilon_2(\vec{k}, \omega_p) = (1.8\times10^{-2})(k/k_0)^2 \quad \text{with static screening}$$

$$= (5.6\times10^{-1})(k/k_0)^2 \quad \text{without screening,}$$

while the results using the asymptotic forms (19) and (20) are

$$\epsilon_2(\vec{k}, \omega_p) = (3.4\times10^{-2})(k/k_0)^2 \quad \text{with screening}$$

$$= (7.4\times10^{-1})(k/k_0)^2 \quad \text{without screening.}$$

The experimental value calculated from the plasmon width is[3]

$$\epsilon_2(\vec{k}, \omega_p) = [(2.7\pm0.9)\times10^{-1}](k/k_0)^2 .$$

As is to be expected, the screening is overestimated by the assumption of static screening and our result is smaller than that of DK, which retains dynamic screening. However, the discrepancy is still less than a factor of 2. The experimental result is bracketed by the screened and unscreened calculation and it is possible that in real metals the damping must be accounted for by mechanisms other than electron correlations such as umklapp processes, impurity scattering, or interband effects.

The smallest electron density for which comparison with DK is possible corresponds to potassium. The results of DK were

$$\epsilon_2(\vec{k}, \omega_p) = (2.5\times10^{-2})(k/k_0)^2 \quad \text{with dynamic screening}$$

$$= 1.6(k/k_0)^2 \quad \text{unscreened.}$$

Our results using the Monte Carlo method and (9) and the asymptotes (19) and (20) are shown in Fig. 4. At the plasmon frequency we find

$$\epsilon_2(\vec{k}, \omega_p) = (2.0\times10^{-2})(k/k_0)^2 \quad \text{with static screening}$$

$$= 0.93(k/k_0)^2 \quad \text{unscreened.}$$

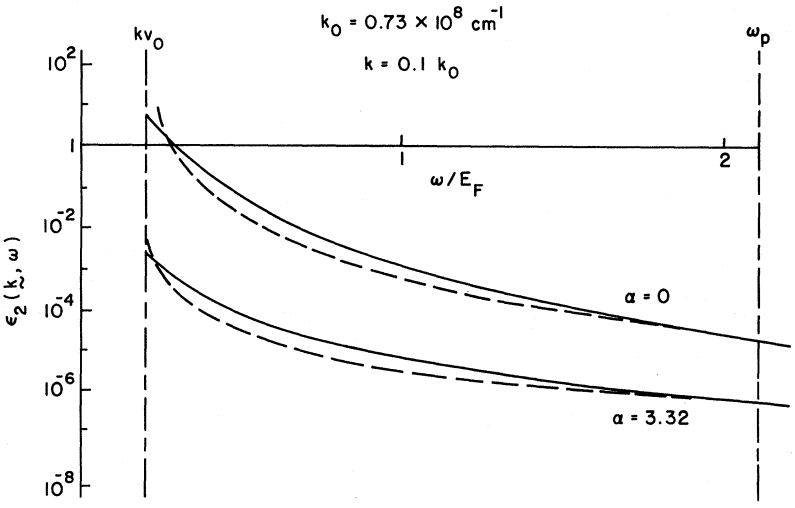

FIG. 4. Imaginary part of the dielectric constant is plotted as a function of ω/E_F for $k_0 = 0.73\times10^8$ cm^{-1} (appropriate to potassium) and $k = 0.1k_0$. The dielectric constant is in units of $2k_0/a_0k^2$. The upper pair of curves are the results of screening ($\alpha = 0$) and the lower pair are the results including Thomas-Fermi screening (in units of k_F^2). Dashed lines represent the results of evaluating (9) by means of a Monte Carlo technique, while the solid lines are the asymptotic formulas (19) and (20).

The differences between the results using static and dynamic screening appear to be even smaller at low electron densities. Since our ansatz is identical to that of DK in absence of screening, the differences between our results and those of DK in the unscreened case are either due to the different numerical procedures employed in evaluating the integrals or to the difficulty in determining $\epsilon_2(\vec{k}, \omega_p)$ from the graph in DK.

As may be seen from Figs. 3 and 4 the asymptotic formulas agree quite well with the more detailed calculation for frequencies greater than twice the Fermi energy. The asymptote also fits well even for relatively low frequencies, though there is no *a priori* reason to expect it to be very good in that region. Consequently, Eqs. (19) and (20) may be used as interpolation formulas or to give order-of-magnitude estimates of the damping for frequencies as low as the Fermi energy. Such an approximation is desirable since the numerical calculation is quite difficult even with static screening. For very high frequencies where screening becomes unimportant the kinematic approximations assumed in deriving the asymptotic forms become exact and the closed form (19) gives the correct result for damping due to electron correlations.

ACKNOWLEDGMENT

A portion of this work was carried out while one of the authors (A. J. G.) was at the Aspen Center for Physics. He would like to thank the Center for its hospitality during this period.

*Supported in part by the U. S. Air Force under Grant No. AF-AFOSR 68-1439, and by National Science Foundation Science Development Grant No. GU 2061.

[1]See, e.g., D. Pines and P. Nozières, *The Theory of Quantum Liquids* (Benjamin, New York, 1966), Vol. I.

[2]D. F. DuBois, Ann. Phys. (N.Y.) 8, 24 (1959).

[3]B. W. Ninham, C. J. Powell, and N. Swanson, Phys. Rev. 145, 209 (1966).

[4]D. F. DuBois and M. G. Kivelson, Phys. Rev. 186, 409 (1969).

[5]A. J. Glick, in *Lectures on the Many-Body Problem*, edited by E. Caianiello (Academic, New York, 1962).

[6]J. Lindhard, Kgl. Danske Videnskab. Selskab, Mat.-Fys. Medd. 28, 8 (1954).

[7]A. J. Glick, Phys. Rev. 129, B99 (1963).

[8]Y. Osaka, J. Phys. Soc. Japan 17, 547 (1962).

[9]D. J. W. Geldart and S. H. Vosko, Can. J. Phys. 44, 2137 (1966).

[10]Notation follows that of Ref. 7.

[11]For a proof and discussion of the relevant theorems see W. F. Long and J. S. Kovacs, Progr. Theoret. Phys. (Kyoto) 44, 952 (1970).

[12]F. Cerulus and R. Hagedorn, Nuovo Cimento Suppl. 9, 646 (1958).

PHYSICAL REVIEW B_1 VOLUME 4, NUMBER 10 15 NOVEMBER 1971

Valence-Band Parameters in Cubic Semiconductors

P. Lawaetz*
Bell Telephone Laboratories, Murray Hill, New Jersey 07974
(Received 15 July 1971)

A five-level $\vec{k}\cdot\vec{p}$ analysis is used to compute the principal effective-mass parameters at $k=0$ in diamond- and zinc-blende-type semiconductors. A semiempirical model is developed to describe the dependence of the momentum matrix elements on lattice constant, ionicity, and d-electron shells in the cores. Satisfactory agreement with available experimental data is achieved with six fitted parameters.

I. INTRODUCTION

A number of important semiconductor properties require for their analysis quite detailed knowledge of effective-mass values at the principal band extrema, but even for some of the most well-known materials it is at present rather difficult to make the best choice from the wealth of experimental and theoretical data existing in the literature. It should also be emphasized that even though simple formal expressions for the effective-mass parameters can readily be obtained from second-order $\vec{k}\cdot\vec{p}$ perturbation theory, the input parameters, notably the momentum matrix elements, have not been known with an accuracy sufficient to render the existing theoretical results reasonably reliable. The reason for this is connected with the fact that most of the theoretical work has stressed other aspects of the band structure, and, as shown recently for Si by Kane,[1] current methods of band-structure calculation may fit the over-all band structure while giving rather unsatisfactory values for the band-edge masses.

In the present work we propose a new procedure for evaluating the interband momentum matrix elements at $\Gamma(k=0)$. Otherwise, our effective-mass calculation is similar to that given by Cardona[2] except for a few details. Based on earlier observa-